

Investigation on Fluid Flow and Heat Transfer Characteristics in Spray Cooling Systems Using Nanofluids

D. H. Lee, Nur Irmawati

Abstract—This paper aims to study the heat transfer and fluid flow characteristics of nanofluids used in spray cooling systems. The effect of spray height, type of nanofluids and concentration of nanofluids are numerically investigated. Five different nanofluids such as AgH_2O , Al_2O_3 , CuO , SiO_2 and TiO_2 with volume fraction range of 0.5% to 2.5% are used. The results revealed that the heat transfer performance decreases as spray height increases. It is found that TiO_2 has the highest transfer coefficient among other nanofluids. In dilute spray conditions, low concentration of nanofluids is observed to be more effective in heat removal in a spray cooling system.

Keywords—Numerical simulation, Spray cooling, Heat transfer, Nanofluids.

I. INTRODUCTION

COOLING is the process of removing thermal energy from a system to bring its temperature down to an acceptable range. The rapid development of complex modern technological and industrial applications such as electronic cooling, combustion technology, biomedical and metallurgical processes demands a high heat flux cooling techniques. Due to the relatively small thermal properties of air, conventional air cooling systems needs to be replaced with liquid spray cooling systems to remove large amounts of heat effectively. Spray cooling occurs when a liquid jet breaks into a fine scattering of droplets when it is forced through a small orifice in a nozzle. These spray droplets will impinge on a heated surface, spread to form a thin liquid film on the surface and evaporate. Inside this thin boundary layer, bubbles will eventually form at the nucleation sites. The impact of more incoming droplets will further interact within the film causing an increase in heat transfer coefficients in the spray cooled zones.

With the recent developments of nanoparticle suspension, an enhancement of water thermal conductivity and heat transfer coefficients is now possible. These nanoparticle suspensions are usually made of metal oxides, carbide and nitride ceramics mixed in base fluids such as water, ethylene glycol and oil. In recent years, there have been increases in interest of nanofluids as heat transfer coefficient is doubled in convective heat applications. Therefore, in order to cope with

demand of higher heat flux technologies, nanofluids can be used in spray cooling technologies to remove a higher amount of heat effectively. For spray cooling of flat surfaces, many researchers have agreed upon that there are four major heat transfer mechanisms involved [1]-[3]. The heat transfer mechanisms are thin liquid film evaporation, droplet impingement resulting in forced convection, nucleation sites on heated surface and secondary nucleation sites on surface of spray droplets.

When the liquid droplets of the spray impinge the heated surface, a thin film of few hundred microns (300-500 μm) will coat the surface and evaporate to remove the heat conducted. Moreover, the incoming droplets force will enhance forced convection speed of liquid flow over the heated surface to replace the hotter liquid film with colder liquid thus promoting the heat flux of a system. Additionally, cavitations on the heated surface acts as the nucleation sites for bubbles to grow as heat that absorbed from the surface. In the presence of forced convection, bubbles are removed more frequently at the nucleation site thus reduces the time interval for another bubble to form on the same site thus increases the heat transfer performance. Besides that, the upper surface of bubbles tends to break into smaller droplets at the top of the liquid film and entraps surrounding vapor which becomes secondary nucleation sites to grow new bubbles.

In the past decade, many researchers have investigated the heat transfer characteristics of water spray cooling systems. A study conducted by [4] has found that an increase in spray pressure would increase the heat transfer performance. This is due to the increase in spray coverage area and mean droplet impact velocity. This is also due to reduction of liquid film thickness. In terms of spray flow rate, researchers have agreed that heat transfer performance is enhanced as spray flow rate increases. Experimental results by numerous researchers [3], [5]-[7] have revealed that an improvement up to 230% at a higher spray flow rate which able to enhance the forced convection effect and number of nucleation sites. Experimental studies using salt solutions and nanofluids have also been conducted by past researchers [5], [6], [8], [9] at various concentrations of nanofluid. They were observed that heat transfer coefficient increases approximately 30% as mixing of the liquid film layer increases.

This paper presents the study of the fluid flow and heat transfer characteristics using nanofluids in spray cooling systems. The nanofluids used in this study include AgH_2O , Al_2O_3 , CuO , SiO_2 and TiO_2 with volume fraction range of

D. H. Lee is with the Department of Mechanical Engineering, Universiti Tenaga Nasional.

Nur Irmawati is with the Department of Mechanical Engineering, Universiti Tenaga Nasional (phone: 03-89217295; e-mail: Irmawati@uniten.edu.my).

0.5% to 2.5%. Results of interest such as heat transfer coefficient and velocity contour are reported to illustrate the effect of spray height, type of nanofluids and nanofluid concentration on the heat transfer coefficient of a spray cooling system.

II. PROBLEM DESCRIPTION AND GOVERNING EQUATIONS

The boundary conditions of the flow domain are illustrated in Fig. 1. The velocity inlet for air is positioned at the top left of the flow above the heated plate. For the water flow outlet, pressure outlet boundary is applied to the vertical and horizontal edges excluding the velocity inlet boundary.

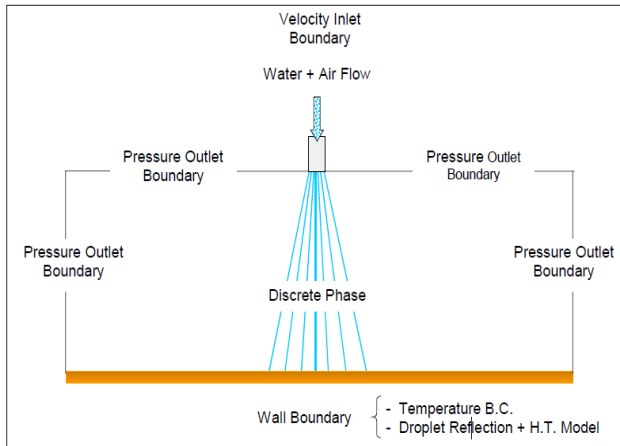


Fig. 1 Water spray cooling model boundary conditions [8]

The steady state and 3D governing conservation equations for the physical problem in this study can be written in dimensionless form as:

Continuity equation:

$$\frac{\partial \rho}{\partial t} + \frac{\partial(\rho u)}{\partial x} + \frac{\partial(\rho v)}{\partial y} + \frac{\partial(\rho w)}{\partial z} = 0 \quad (1)$$

X-momentum equation:

$$\rho \frac{du}{dt} = \frac{\partial(-p + \tau_{xx})}{\partial x} + \frac{\partial \tau_{yx}}{\partial y} + \frac{\partial \tau_{zx}}{\partial z} + S_{Mx} \quad (2)$$

Y-momentum equation:

$$\rho \frac{dv}{dt} = \frac{\partial \tau_{xy}}{\partial x} + \frac{\partial(-p + \tau_{yy})}{\partial y} + \frac{\partial \tau_{zy}}{\partial z} + S_{My} \quad (3)$$

Z-momentum equation:

$$\rho \frac{dw}{dt} = \frac{\partial \tau_{xz}}{\partial x} + \frac{\partial \tau_{yz}}{\partial y} + \frac{\partial(-p + \tau_{zz})}{\partial z} + S_{Mz} \quad (4)$$

Energy equation:

$$\frac{dE}{dt} = -div(pu) + \left(\frac{\partial(u\tau_{xx})}{\partial x} + \frac{\partial(u\tau_{yx})}{\partial y} + \frac{\partial(u\tau_{zx})}{\partial z} \right) + \left(\frac{\partial(v\tau_{xy})}{\partial x} + \frac{\partial(v\tau_{yy})}{\partial y} + \frac{\partial(v\tau_{zy})}{\partial z} \right) + \left(\frac{\partial(w\tau_{xz})}{\partial x} + \frac{\partial(w\tau_{yz})}{\partial y} + \frac{\partial(w\tau_{zz})}{\partial z} \right) + div(k \cdot grad T) + S_E \quad (5)$$

In above governing equations, the following equations were used to calculate the thermophysical properties of nanofluids as given by [9]:

The density of the nanofluids:

$$\rho_{nf} = (1 - \phi)\rho_f + \phi\rho_s \quad (6)$$

The specific heat of the nanofluids:

$$(\rho c_p)_{nf} = (1 - \phi)(\rho c_p)_{bf} + \phi(\rho c_p)_{np} \quad (7)$$

The dynamics viscosity of the nanofluids:

$$\mu_{nf} = \mu_{bf}(1 + 2.5\phi) \quad (8)$$

The thermal conductivity of the nanofluids:

$$k_{nf} = \frac{k_{np} + 2k_{bf} + 2(k_{np} - k_{bf})\phi}{k_{np} + 2k_{bf} - (k_{np} - k_{bf})\phi} \cdot k_{bf} \quad (9)$$

The latent heat of vaporization of the nanofluids:

$$(\rho h_{fg})_{nf} = (1 - \phi)(\rho h_{fg})_{bf} + IMF \cdot \phi(\rho h_{fg})_{np} \quad (10)$$

where

$$IMF = \frac{T_{b,bf}}{T_{b,nf}} \quad (11)$$

III. RESULTS AND DISCUSSIONS

A. Velocity Contour

The velocity contour for various spray height is depicted in Figs. 2 (a)-(e). It is observed that as the spray height increases, the spray coverage area increases but the thickness and velocity of the wall film decreases. This signifies that the wall film velocity is decreasing with an increase in spray height. This is because energy is lost by the spray droplets to overcome the vaporized liquid over a longer travelling distance. Therefore, the impingement velocity of the spray droplets is considerably reduced causing a drop in convective heat transfer and overall heat transfer performance.

The velocity contour for various nanofluid concentrations is shown in Figs. 3 (a)-(e). It can be observed that the spray flow becomes more turbulent as the nanofluid concentration increases. The swirling particle tracks are found to increase in density as the concentration of nanofluid increases. This is due to the greater amount of nano-sized suspensions in the fluid which collides with each other more frequently thus resulting in a highly turbulent flow. Moreover, the wall film formed increases in thickness and turbulence as it moves radially outwards as expected of a standard spray cooling system.

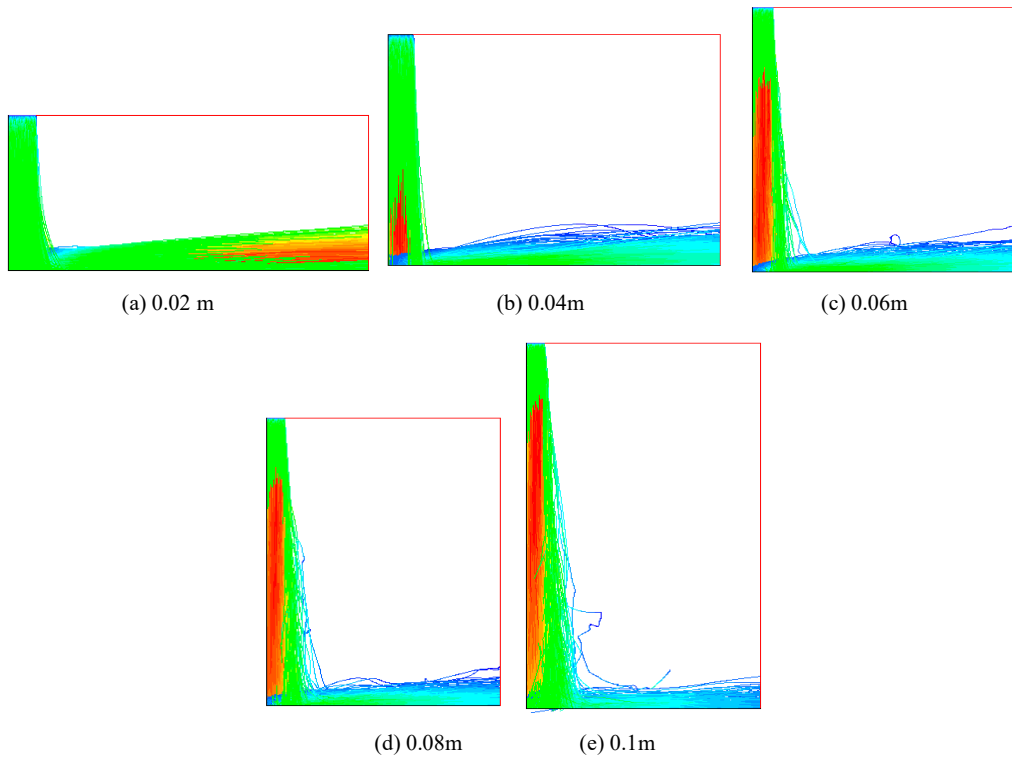


Fig. 2 Spray velocity contour for various spray heights

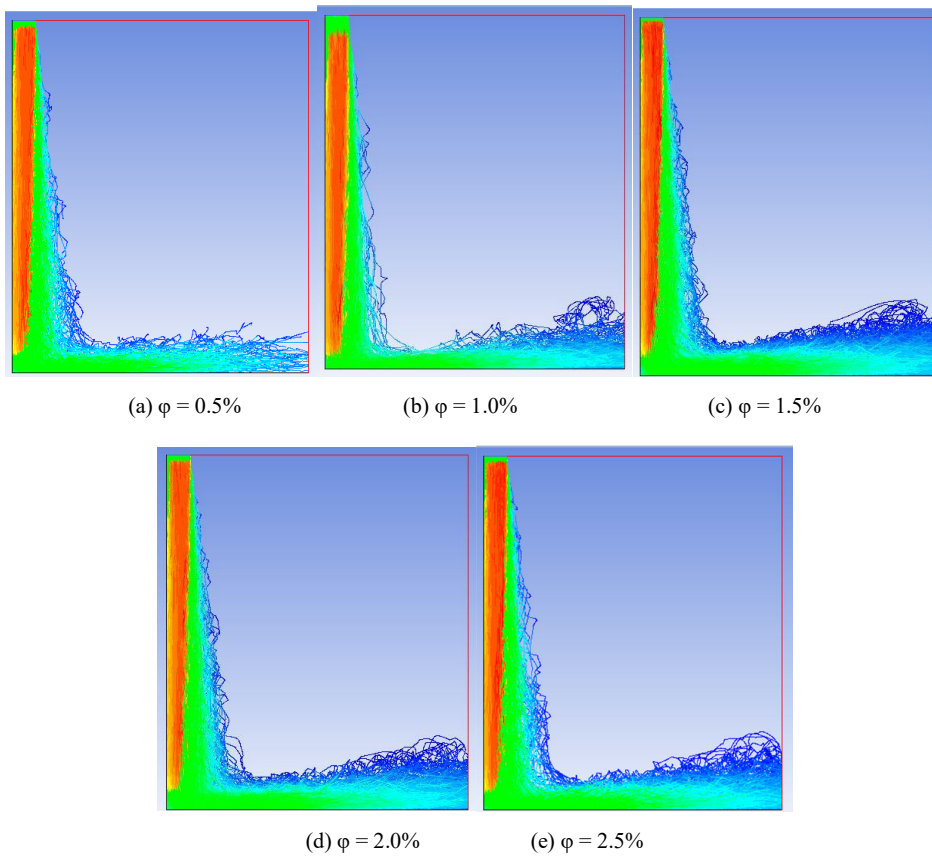


Fig. 3 Spray velocity contour various nanofluids concentrations

B. Heat Transfer Coefficient

The maximum heat transfer coefficient of each spray height has been extracted and plotted as shown in Fig. 4. It is noted that the heat transfer coefficient increases until a peak at an optimum spray height of 0.06 m before decreasing. This is because as the spray height increases, the droplets momentum and energy reduces to overcome the uprising vapor flow causing loss in impact velocity. Moreover, the formation of stagnation pool in the middle of the spray cone also affects the heat transfer performance. These negative effects will cancel out the heat transfer enhancement due to the increase in coverage area thus reduces the overall heat transfer coefficient of the spray cooling model. Therefore, the optimum spray height of this research model is found to be 0.06 m.

Fig. 5 shows the heat transfer coefficient along the heated wall surface for various types of nanofluids and water. It is observed that the application of nanofluids as the spray coolant have increased the heat transfer coefficient when compared to water spray cooling. This increase in heat transfer coefficient is noted in all five of the nanofluids TiO_2 is performing the best. Based on the results obtained, the maximum heat transfer coefficient and the percentage of increase as compared to water for all nanofluids are tabulated in Table I. TiO_2 with 1% concentration recorded the maximum improvement of 32.64% followed by SiO_2 , CuO , Al_2O_3 and AgH_2O . This increase in heat transfer coefficient is due to the addition of the high thermal conductivity nanoparticles in the nanofluids. As noted previously, the addition of nanoparticles results in more turbulent fluid flow which increases the convective heat transfer. Besides that, these nanoparticles also have the ability to conduct more heat than water molecules during the short time of contact with the heated surface due to its higher thermal conductivity. In dilute spray conditions, these low concentrations nanoparticles will be able to rebound directly from the heated surface without adhering to it. After absorbing a large amount of heat, it will be washed away by subsequently arriving droplets thus removing a higher amount of heat than pure water spray coolant conditions. Therefore, it can be said that the combination of the occurrence of these scenarios contributed to the general increase in heat transfer performance of nanofluid spray cooling.

TABLE I
MAXIMUM HEAT TRANSFER COEFFICIENT AND INCREASE PERCENTAGE OF COOLANTS

Material	Heat Transfer Coefficient ($\text{W}/\text{m}^2\text{K}$)	Percentage of Increase (%)
Water	2819.23	-
AgH_2O	3301.62	17.11
Al_2O_3	3360.47	19.20
CuO	3500.71	24.17
SiO_2	3653.01	29.57
TiO_2	3739.3	32.64

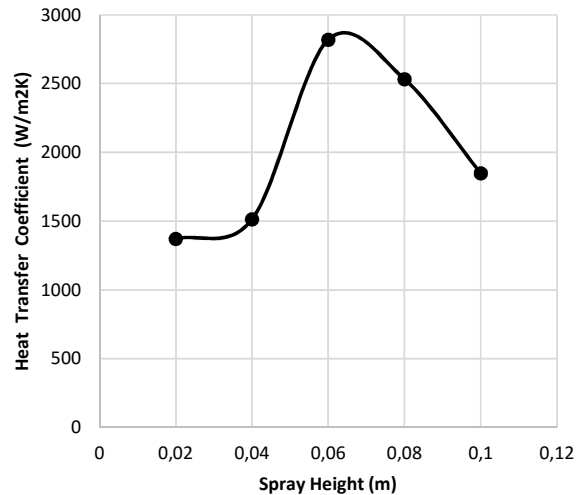


Fig. 4 The heat transfer coefficient againsts spray height

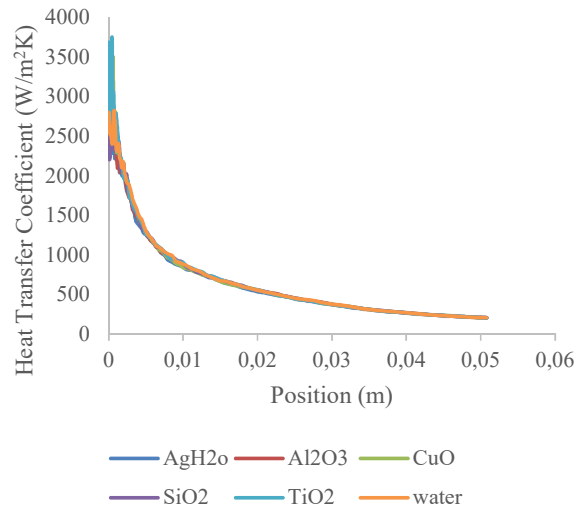


Fig. 5 The heat transfer coefficient across the heated wall surface for various types of nanofluids

The maximum heat transfer coefficient of each nanofluid concentration has been extracted and plotted as shown in Fig. 6. As this figure shows, the heat transfer coefficient decreases with an increase in nanofluid concentration. This is due to as the spray concentration increases; there are an abundance of nanoparticles which promotes the deposition of the material on the heated surface. The formation of an irregular shaped nano-sorption layer reduces the wettability of the surface thus reducing the number of nucleation points. Therefore, the convective heat transfer mechanism is inhibited thus lowering the heat transfer efficiency. Another reason for the decrease in heat transfer performance is due to the far too short impingement time of the nanoparticle with the heated surface. The impingement time is the amount of time available for heat transfer to take place when the nanoparticle is in contact with

the heat sources. Due to the increase in turbulence, the nanoparticles may not be in contact with the heat source for a long enough period of time to effectively transfer the desirable amount of heat. Therefore, most of the nanofluid would be washed away by subsequent droplets without being heated up.

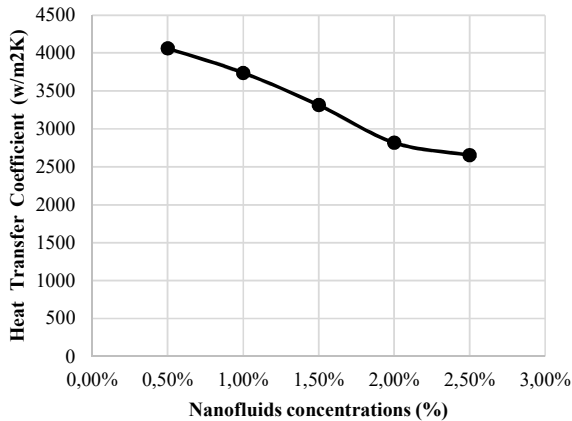


Fig. 6 The heat transfer coefficient for various nanofluids concentrations

IV. CONCLUSIONS

Numerical investigation on the fluid flow and heat transfer characteristics of nanofluids in spray cooling systems are reported. It is deduced that heat transfer coefficient increases until a peak as spray height increases and decreases drastically with any further increase after the optimum spray height. The optimum spray height in the current study was found to be 0.06 m. The effect of different types of nanofluids such as AgH₂O, Al₂O₃, CuO, SiO₂ and TiO₂ on heat transfer coefficient have been investigated. It is found that TiO₂ has the most effective heat transfer rate with the highest improvement of 32.64%. Moreover, the heat transfer coefficient decreases as the nanofluid concentration increases.

REFERENCES

- [1] J. Kim, Spray cooling heat transfer: The state of the art, *International Journal of Heat and Fluid Flow*, Bd. 28, pp. 753 - 767, 2007.
- [2] A. Marcos, L. C. Chow, J. H. Du, S. Lei, D. P. Rini and J. J. Lindauer, *Spray Cooling At Low System Pressure*, 18th IEEE SEMI-THERM Symposium, 2002.
- [3] Z. Yan, R. Zhao, F. Duan, T. N. Wong, K. C. Toh, K. F. Choo, P. K. Chan and Y. S. Chua, „Spray Cooling,“ in *Two Phase Flow, Phase Change and Numerical Modelling*, Temasek, InTech, 2011, pp. 287 - 307.
- [4] S. Somasundaram und A. A. O. Tay, A Study of the Effect of Exit Boundary Conditions on the Performance of a Spray Cooling System, 12 *Electronics Packaging Technology Conference*, 2010.
- [5] T. B. Chang, S. C. Syu und Y. K. Yang, Effects of particle volume fraction on spray heat transfer performance of Al₂O₃ - water nanofluid, *International Journal of Heat and Mass Transfer*, Bd. 55, pp. 1014-1021, 2012.
- [6] Q. Cui, S. Chandra und S. McCahan, The effect of dissolving salts in water sprays used for quenching a hot surface: Part 2 - Spray cooling, *Heat Transfer*, Bd. 125, pp. 333 -337, 2003.
- [7] K. Choo, Z. Yan, K. Toh, F. Duan und T. Wong, Heat transfer characteristics of impingement spray cooling system for electronic test cards, *IEEE*, Bd. 5, pp. 326 -329, 2010.
- [8] C. Yiğit, N. Sözbir, S. C. Yao, H. R. Güven und R. J. Issa, Experimental measurements and computational modeling for the spray cooling of a steel plate near the Leidenfrost temperature, *Journal of Thermal Science and Technology*, Bd. 31, Nr. 1, pp. 27-36, 2011.
- [9] O. Manca, S. Nardini, D. Ricci und S. Tamburrino, Numerical Investigation on Mixed Convection in Triangular Cross-Section Ducts with Nanofluids, *International Journal of Heat and Fluid Flow*, Bd. 110, pp. 1082-1096, 2012.